Ecological Engineering 59 (2013) 167–175

Contents lists available at ScienceDirect

Ecological Engineering

journal homepage: www.elsevier.com/locate/ecoleng

Vegetation dynamics in response to water inflow rates and fire in a brackish *Typha domingensis* Pers. marsh in the delta of the Colorado River, Mexico

Lourdes Mexicano[a,*], Pamela L. Nagler[b], Francisco Zamora-Arrroyo[c,d], Edward P. Glenn[a]

[a] Department of Soil, Water and Environmental Science, University of Arizona, Tucson, AZ 85726, USA
[b] U.S. Geological Survey, Sonoran Desert Research Station, University of Arizona, Tucson, AZ 85726, USA
[c] Sonoran Institute, Tucson, AZ 85701, USA
[d] Environmental Research Laboratory of the University of Arizona, 2601 East Airport Drive, Tcuson, AZ 85706, USA

ARTICLE INFO

Article history:
Received 13 April 2012
Received in revised form 13 June 2012
Accepted 23 June 2012
Available online 23 July 2012

Keywords:
Emergent wetland
Cattail marsh
Brackish
Fire effects
Quickbird
MODIS
Remote sensing

ABSTRACT

The Cienega de Santa Clara is a 5600 ha, anthropogenic wetland in the delta of the Colorado River in Mexico. It is the inadvertent creation of the disposal of brackish agricultural waste water from the U.S. into the intertidal zone of the river delta in Mexico, but has become an internationally important wetland for resident and migratory water birds. We used high resolution Quickbird and WorldView-2 images to produce seasonal vegetation maps of the Cienega before, during and after a test run of the Yuma Desalting Plant, which will remove water from the inflow stream and replace it with brine. We also used moderate resolution, 16-day composite NDVI imagery from the Moderate Resolution Imaging Spectrometer (MODIS) sensors on the Terra satellite to determine the main factors controlling green vegetation density over the years 2000–2011. The marsh is dominated by *Typha domingensis* Pers. with *Phragmites australis* (Cav.) Trin. Ex Steud. as a sub-dominant species in shallower marsh areas. The most important factor controlling vegetation density was fire. Spring fires in 2006 and 2011 were followed by much more rapid green-up of *T. domingensis* in late spring and 30% higher peak summer NDVI values compared to non-fire years ($P < 0.001$). Fires removed thatch and returned nutrients to the water, resulting in more vigorous vegetation growth compared to non-fire years. The second significant ($P < 0.01$) factor controlling NDVI was flow rate of agricultural drain water from the U.S. into the marsh. Reduced summer flows in 2001 due to canal repairs, and in 2010 during the YDP test run, produced the two lowest NDVI values of the time series from 2000 to 2011 ($P < 0.05$). Salinity is a further determinant of vegetation dynamics as determined by greenhouse experiments, but was nearly constant over the period 2000–2011, so it was not a significant variable in regression analyses. It is concluded that any reduction in inflow volumes will result in a linear decrease in green foliage density in the marsh.

1. Introduction

1.1. Importance of Cienega de Santa Clara as a remnant wetland in the Colorado River delta

The Colorado River delta in Mexico historically supported several hundred thousand hectares of wetland and riparian habitat (Glenn et al., 2001). Due to construction of upstream dams and the diversion of water for agriculture and urban uses in the U.S. and Mexico, river flows to the delta are much diminished (Nagler et al., 2009a,b). A bright spot in this picture is Cienega de Santa Clara, a large (ca. 5600 ha) emergent marsh in the eastern portion of the delta (Fig. 1) (Glenn et al., 1992; Zengel et al., 1995) This anthropogenic wetland was created starting in 1977 by the discharge of saline agricultural drain water from the Wellton-Mohawk Irrigtion District in the U.S. to the north end of the Santa Clara Slough in Mexico, an area of former mudflats in the intertidal zone of the river. The primary plant species in the Cienega is southern cattail (*Typha domingensis* Pers.), with common reed (*Phragmites australis* (Cav.) Trin. ex Steud.) colonizing shallower areas within the *Typha* stands (Fig. 2) (Zengel et al., 1995). The Cienega is included in the core area of the Biosphere Reserve of the Upper Gulf of California and Delta of the Colorado River, and supports numerous species of resident and migratory water birds, as well as other wildlife (Zengel et al., 1995; Zengel and Glenn, 1996; Hinojosa-Huerta et al., 2001, 2002). It supports 80% of the remaining Yuma clapper rails, a listed endangered species in both the U.S. and Mexico (Hinojosa-Huerta et al., 2001, 2002).

* Corresponding author. Tel.: +1 520 3038795.
E-mail address: cliomex@yahoo.com (L. Mexicano).

0925-8574/$ – see front matter © 2012 Elsevier B.V. All rights reserved.
http://dx.doi.org/10.1016/j.ecoleng.2012.06.046

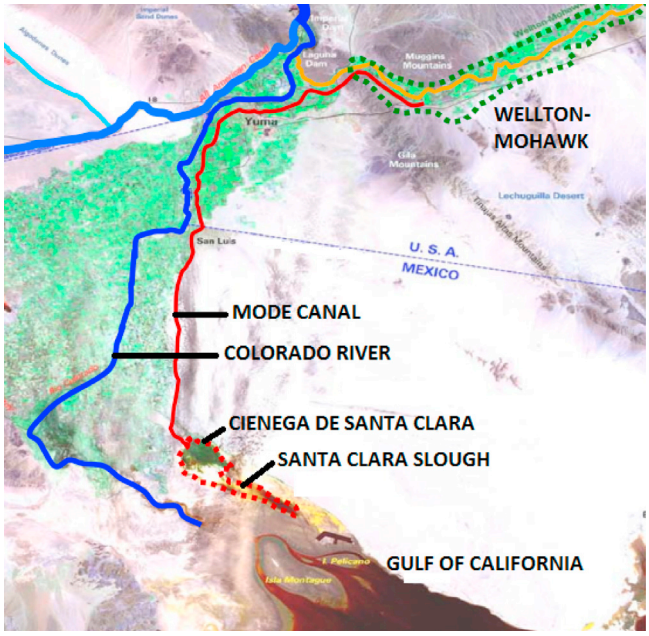

Fig. 1. Locator map showing Wellton-Mohawk Irrigation District, the origin of water flowing to Cienega de Santa Clara in the MODE canal.

1.2. Rationale for the study

Water flows to the Cienega are not guaranteed (Gabriel and Kelli, 2010); in fact, the Cienega was the inadvertent creation of the 1974 Colorado River Basin Salinity Control Act in the U.S. (Glenn et al., 1992). Before this act was passed, Wellton-Mohawk drain water was delivered to Mexico in the Colorado River as part of their allotment of Colorado River water. However, the brackish water caused salinity problems in Mexican agricultural fields, and the U.S. pledged to replace Wellton-Mohawk drainage with higher quality water, and to build the Yuma Desalting Plant (YDP) to ultimately desalinize the Wellton-Mohawk drainage water for delivery to Mexico. The Main Outlet Drain Extention (MODE) canal was built to convey drainage water to the intertidal zone of the Gulf of California while the plant was under construction, and ultimately to receive reverse-osmosis effluent brine from the YDP. However, due to delays and lack of funding, the YDP has only operated during brief test runs: at 33% capacity for 6 months in 1993; at 10% capacity for 3 months in 2007; and at 30% capacity for12 months in 2010–2011. Except during test runs of the YDP, flows to the Cienega have averaged about 4 m s^{-1} at a salinity of 2.8 g L^{-1} total dissolved solids since the MODE became operational (Garcia-Hernandez et al., 2000; Huckelbridge et al., 2010). As a result of these discharges, an internationally important wetland has been created.

Fig. 2. Aerial photograph taken by Francisco Zamora-Arroyo in January, 2010, showing green *Phragmites australis* amidst dormant *Typha domingensis* in the Ciénega de Santa Clara.

The present study was part of a monitoring program designed to detect effects of the YDP on the Cienega during the test run in 2010–2011. The objectives of this study were: (1) map vegetation in the Cienega before, during and after the test run of the YDP to determine effect of plant operation on the marsh vegetation; (2) determine longer term trends in vegetation dynamics in response to inflows, salinity and fire events; and (3) identify the main factors controlling vegetation extent and green foliage density in the Cienega. The overall goal was to contribute to the development of management tools for those agencies and stakeholders charged with maintaining the environmental values of the Cienega while meeting treaty obligations to provide water to Mexico. The research combined ground data with satellite imagery, including high resolution images for detailed vegetation mapping (Quickbird and WorldView-2) and high-frequency, moderate resolution images for detecting vegetation dynamics over time, using the Moderate Resolution Imaging Spectrometer (MODIS) sensors on the Terra satellite. Combining high-spatial-resolution imagery to create vegetation maps with high-temporal-resolution imagery to detect phenological changes in vegetation can be more powerful change-detection tools than either type of imagery alone (e.g., Lunetta et al., 2006).

1.3. Approach to vegetation mapping

Several approaches to vegetation mapping with satellite imagery have been developed (Muller, 1997; Jensen, 2000; Nagler et al., 2005; reviewed in Xie et al., 2008). For example, vegetation types can sometimes be differentiated based on spectral properties, using either supervised or unsupervised classification programs in which satellite bands are combined to produce unique signatures for each vegetation type. Another approach is for trained interpreters to divide the image into polygons representing different vegetation types based on expert opinion. In the present study, there were only two major vegetation types and their locations were stable, and our main interest was in detecting changes in green vegetation density over time. Therefore, we developed an approach based on the Normalized Difference Vegetation Index (NDVI) (Pettorelli et al., 2005). NDVI is calculated as:

$$\rho\mathrm{NDVI} = \frac{\rho\mathrm{NIR} - \rho\mathrm{Red}}{\rho\mathrm{NIR} + \rho\mathrm{Red}} \quad (1)$$

where ρNIR and ρRed are reflectance values in red and near-infrared sensor bands. NDVI reduces the image to a single layer with NDVI values from −1.0 to +1.0, with water having strongly negative values, soils slightly negative to slightly positive, and vegetation having positive values (Jensen, 2000; Glenn et al., 2008).

NDVI of vegetation is strongly sensitive to chlorophyll absorption of Red and scattering and reflection of NIR by cell walls and stacked layers of cells in leaves, and provides a measure of canopy "greenness" (Glenn et al., 2008). Vegetation indices have been highly successful in assessing vegetation condition, foliage, cover, phenology, and processes such as evapotranspiration (ET) and

Table 1
Sensor and satellite specificiations for Quickbird (Digital Globe, Inc., 2006), WorldView-2 (Updike and Comp, 2010) and MODIS (Huet et al., 2011) imagery.

Attribute	Quickbird	WorldView-2	MODIS
Panchromatic resolution			NA
Spectral	450–900 nm	450–800 nm	
Spatial	0.61 m at Nadir, 1.14 m at 45° Off Nadir	0.46 m at Nadir, 0.52 m at 20° Off Nadir	
Red Band resolution			
Spectral	630–690 nm	630–690 nm	620–670 nm
Spatial	2.44 m at Nadir, 4.56 m at 45° Off Nadir	1.84 m at Nadir, 2.08 m at 20° Off Nadir	250 m
NIR band resolution			
Spectral	760–900 nm	770–895 nm	841–876 nm
Spatial	2.44 m at Nadir, 4.56 m at 45° Off Nadir	1.84 m at Nadir, 2.08 m at 20° Off Nadir	250 m
Altitude	450 km	770 km	705 km
Swath width	16.5 km at Nadir	16.4 km at Nadir	2330 m at Nadir
Equator cross time	10:30 am	10:30 am	10:30 am

primary productivity, related to the fraction of photosynthetically active radiation absorbed by a canopy (Glenn et al., 2008; Kerr and Ostrovsky, 2003; Pettorelli et al., 2005). Vegetation indices are robust satellite data products computed the same way across all pixels in time and space, regardless of surface conditions. As ratios, they can be easily cross-calibrated across sensor systems, ensuring continuity of data sets for long-term monitoring of ecosystems by different satellites and sensor systems (Baldi et al., 2008; Verbesselt et al., 2010).

2. Materials and methods

2.1. Satellite sensors and data sets

Vegetation maps were prepared from high-resolution (ca. 0.5 m resolution) Quickbird or WorldView-2 images (Digital Globe, Inc., Longmont, CO) at approximately quarterly intervals, 2008–2011, while Moderate Resolution Imaging Spectrometer (MODIS) images (ca. 250 m resolution) from the Terra satellite were used to track changes in the Cienega from 2000 to 2011. Satellite sensor specifications are in Table 1 and a list of Quickbird and WorldView-2 images used in the study are in Table 2. The Quickbird and WorldView-2 images covered an area of approximately 20 km × 20 km that encompassed the entire Cienega plus surrounding areas. Quickbird images were supplied as pan-sharpened panchromatic plus four-band multispectral (Blue, Green, Red, NIR) Standard Imagery products with geometric and radiometric corrections. WorldView-2 images were supplied as pan-sharpened panchromatic plus eight-band multispectral Standard Imagery products. Quickbird and WorldView-2 satellites are intercalibrated so satellite data can be used interchangeably. The radiometric corrections applied to these products include relative radiometric response between detectors, non-responsive detector fill, and a conversion for absolute radiometry. The sensor corrections account for internal detector geometry, optical distortion, scan distortion, any line-rate variations, and mis-registration of the multispectral bands (Krause, 2005; Updike and Comp, 2010). Due to the low relief of the target area, ortho-rectification was not needed.

Table 2
High-resolution satellite imagery from Digital Globe, Inc., used in the study of Cienega de Santa Clara. QB, Quickbird; WV, WorldView 2. Cloud cover is percent clouds over the target area. ONA, off-nadir angle.

Date	Image Type	ID No.	Cloud cover (%)	ONA (°)
Sept. 8, 2008	QB	10100100088A9400	0	14.25
Feb. 12, 2009	QB	101001000981AB00	0	4.31
Apr. 25, 2009	QB	101001009871AB00	0	4.31
Aug. 19, 2009	QB	101001000A28001	0	14.25
Jan. 15, 2010	QB	101001000AF21C00	0	19.79
Apr. 2, 2010	WV2	1030010004848700	0	18.37
July 7, 2010	WV2	10300100054CBF00	0	7.72
Apr. 27, 2011	WV2	103001000A72CB00	0	14.73
Oct. 7, 2011	QB	101001000E3FFA00	0	23.97

2.2. Quickbird and WorldView-2 image processing, classification procedures and error analyses

Digital Number (DN) values for Red and NIR bands were converted to at-satellite reflectance values using image-specific data and equations in Krause (2005) for Quickbird and Updike and Comp (2010) for WorldView-2. DN values were first converted into radiance values, then into reflectance values using data on solar zenith angle in the header file and earth–sun distance based on the date of image acquisition. Reflectance-based NDVI images (Eq. (1)) were created using ERDAS Imagine software (Atlanta, GE). The stability of NDVI values across different images was evaluated by plotting mean, maximum and minimum values for each image (Fig. 3); values for mean and maximum NDVI differed by less than 10% among images. Hence, atmospheric effects on NDVI at different acquisition dates were considered to be negligible in this study.

An Area of Interest (AOI) file was created in ERDAS around the perimeter of the Cienega. It had an area of 5635 ha that encompassed the permanently vegetated portion of the marsh plus a buffer zone of areas that were vegetated on some images but not others. This AOI file was applied to each image for analyses of land cover types. NDVI ranges defining land cover classes were

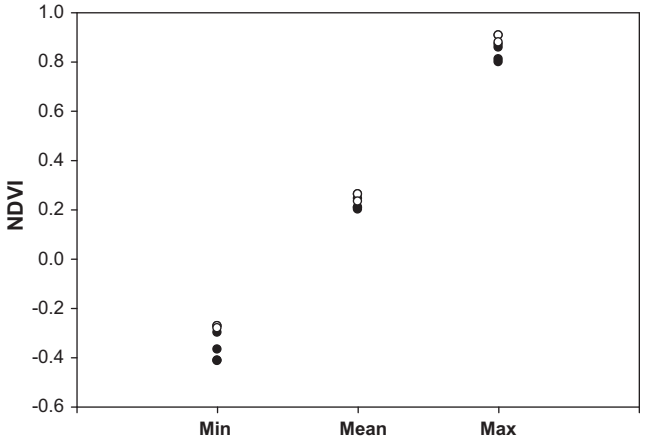

Fig. 3. Stability of NDVI values among Quickbird (QB) (closed circles) and WorldView-2 (WV2) (open circles) images used in producing the seasonal Ciénega vegetation maps. Values are minimum, mean and maximum values for all pixels on each image. Nine points per class were plotted but some symbols overlap.

determined by comparing known land cover types visible on the September 2008 and August 2009 panchromatic Quickbird image with NDVI values of the same features on the NDVI image. In an iterative procedure, we used supervised and unsupervised classification programs in ERDAS to divide the August 2009 image into as many as 20 classes, then we inspected the panchromatic image and aerial photographs to attempt to produce a final set of classes that corresponded to identifiable, stable features on the whole set of images.

Each subsequent NDVI image was then subjected to an unsupervised classification procedure in ERDAS that binned pixels into 12 classes according to the nearest-neighbor algorithm. Then the 12 classes were compressed into the defined classes based on mean NDVI values for each class (see Results). Validation and error analyses were conducted by comparing reference data to classified data on images from February 2009 (Quickbird), July 2010 (WorldView-2) and October 2011 (Quickbird), representing a wide range of vegetation conditions in the marsh. Reference data on each image were collected for individual pixels representing land cover classes that could be unambiguously identified on the images. Reference sites were selected based on visual inspection of the panchromatic images, knowledge from field and aerial surveys of the land cover types at specific locations in and around the Cienega (Greenberg and Schlatter, 2012). From 28 to 113 points were compared for each cover class across images. Water samples were selected in the permanent open-water lagoons within the Cienega and in the shallow pools of water in the outflow areas around the edges of the Cienega. Soil samples were selected in areas of wet and dry bare soil along the edges of the Cienega. Dry vegetation was sampled on the February 2009 image in areas of dormant *T. domingensis*. Different intensities of green vegetation were selected from throughout the marsh based on false-red NIR intensity on multiband images.

Data were entered into an error matrix and analyzed as described in Congalton (1991). For each class a Users Accuracy and a Producers Accuracy was calculated. The Users Accuracy is the percentage of pixels that should have been put into a given class but were not (the percentage correct for a given row divided by the total for that row in the matrix) while the Producers Accuracy represents the percentage of a given class that is correctly identified on the map (the percentage correct for a given column divided by the total for that column). Cohen's unweighted Kappa value (Cohen, 1960) for the overall error matrix was calculated by the formula:

$$\text{Kappa} = \frac{[Pr(a) - Pr(e)]}{[1 - Pr(e)]} \quad (2)$$

where Pr(a) is the relative observed agreement between reference samples and classified data, Pr(e) is the hypothetical probability of change agreement. A Kappa value of 1.0 denotes complete agreement while a Kappa of 0 indicates no agreement above that expected by chance. Kappa was calculated by entering the error matrix data into an on-line calculator (http://vassarstats.net/kappa.html).

2.3. NDVI from MODIS

MODIS has near-daily coverage of most of the earth with about 250 m resolution (Huete et al., 2011). We used the MOD13Q1 NDVI product, which is a composite of 3–5 high quality, cloud-free images selected for each 16-day collection period. Band values are corrected to at-surface reflectance values and vegetation index products are supplied to end-users as pre-processed, validated data sets. MODIS data in this study was obtained from the Oak Ridge National Laboratory DAAC website (http://daac.ornl.gov/cgi-bin/MODIS/GLBVIZ_1_Glb/modis_subset_order_global_col5.pl). We defined a 1600 ha study area (256 MODIS pixels) in the center of the Cienega to study changes in NDVI over time (Fig. 4). This polygon excludes major open water areas in the north and south ends of the Cienega, as water interferes with the NDVI vegetation signal. It also excludes the western edge of the Cienega, which is prone to periodic drying due to buildup of silt in the entry channel; our goal was to pick a stable area of vegetation to detect changes due to variable inflow rates, fires and salinity changes.

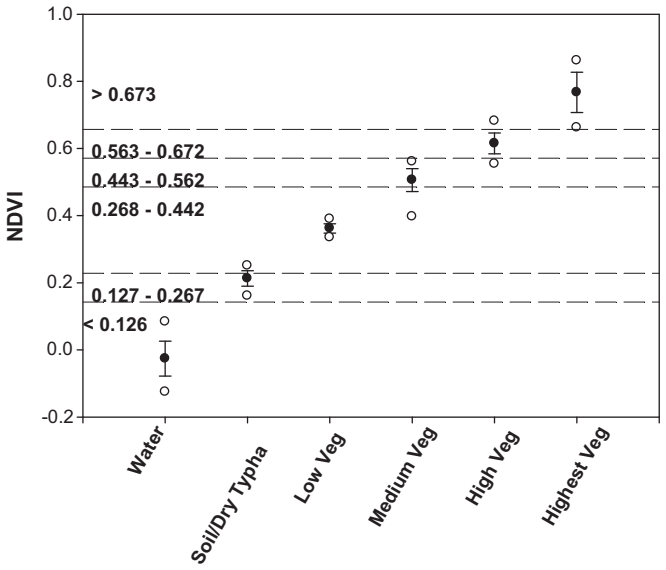

Fig. 4. Footprint of the array of MODIS NDVI pixels selected for analysis of vegetation trends in Cienega de Santa Clara, 2000–2011.

2.4. Ground data sources and regression analyses of NDVI on flow volumes and salinities

Ground surveys of the Cienega were conducted at monthly intervals in 2009–2010 (Greenberg and Schlatter, 2012). Twenty-three sampling stations distributed through the marsh were visited to determine water quality parameters and to assess the state of the vegetation. In addition, an aerial survey was conducted in January 2010, and the vegetation was documented through oblique photography using a hand-held digital camera. Flow data were daily mean values recorded in the MODE canal at the Southerly International Boundary between the U.S. and Mexico by the International Boundary and Water Commission (http://www.ibwc.gov/wad/DDQWMSIB.HTM). Salinity of inflow water were monthly values provided by the same source. The occurrence of major fire events in 2006 and 2011 were based on local observations and verified by obtaining archival Landsat 5 images from the U.S. Geological Survey Earth Explorer website (http://earthexplorer.usgs.gov/). Statistical analyses were performed using Systat, Inc. software (Chicago, IL). Ground observations were based on monthly field observations made before, during and after the period of YDP operation in 2010.

MODIS NDVI data was regressed against MODE inflow volume and salinity data for each year from 2000 to 2011. Although the YDP operated for 12 months in 2010–2011, for most of the year replacement water from other sources in the U.S. and Mexico was discharged into the canal to minimize disturbance to vegetation and wildlife in the Cienega. No replacement water was available for part of the run; flows were markedly reduced and salinities increased from May 9 to September 14, 2010. Therefore, we used

Fig. 5. Distribution of NDVI values in each land cover class defined on Quickbird and WorldView 2 images. The range of NDVI values are shown for the six final land cover classes defined on the training images. Data from validation images are plotted for each class, showing means (closed circles), standard deviations (error bars) and maximum and minimum (open circles) for each class.

this time period each year to compare NDVI among years. Analyses were conducted using Systat software (Longmont, CO).

3. Results

3.1. Error analysis of classification procedure

We initially defined seven land cover classes for analysis corresponding to water, soil, dead or dormant (non-green) vegetation (e.g., *T. domingensis* in winter) and four green vegetation classes. However, NDVI values for soil and dry vegetation overlapped, and an accuracy of only 35% was achieved when attempting to separate these based on NDVI values, even though they were easily distinguished visually on panchromatic images. Hence, soil and dry vegetation were combined into a single NDVI class, and the final six classes were defined based on NDVI ranges from the August 2009 image as shown in Fig. 5. The six final classes selected for validation consisted of: (1) water; (2) soil plus dry (non-green) vegetation (e.g., dormant *Typha*); (3) low-density green vegetation; (4) medium-density green vegetation; (5) high-density green vegetation; and (6) highest-density green vegetation. Means, standard deviations and maximum and minimum values of validation samples are plotted against the target NDVI ranges in Fig. 5. The water class was completely separated from the other classes by NDVI values, but ranges for the other classes tended to overlap. An error matrix is in Table 3. Water could be completely resolved from all other classes. Accuracy of other classes was also high, with an overall Producers Accuracy of 91% and a Users Accuracy of 87% and an overall Kappa value of 0.93. This high accuracy is expected because water, soil and plant litter can generally be resolved from green leaf material by NDVI (e.g., Jensen, 2000; Glenn et al., 2008), and the different classes of green vegetation in this study were defined by their mean NDVI values, hence the only error was introduced by the overlapping ranges of NDVI among classes on different images. However, it was necessary to distinguish between bare soil and dry or dormant vegetation based on context within images rather than on NDVI values.

3.2. Vegetation maps and distribution of land cover classes

T. domingensis is winter dormant, greening up in late April and becoming dormant in November at this location. On the other hand, the sub-dominant species, *P. australis*, is green all year in the Cienega. This offers a means of distinguishing between the two species based on phenology, as *P. australis* appears as green islands amidst dormant *T. domingensis* stands in winter (see Fig. 2).

Fig. 6 illustrates key changes in the vegetation maps over time and Table 1 displays the number of hectares in each cover class on each image. In September 2008 (Fig. 6A) vegetation cover was near it maximum areal extent, but the western edge of the Cienega fell into the low-density vegetation class. This was due to a dry-down of that portion of the marsh due to the deposition of silt in the north end of the marsh. As it crosses Gran Desierto, wind-blown sand enters the canal and it is deposited in the Cienega, requiring periodic dredging to keep the entry point for water and silt into the Cienega open. Between dredging events, the western edge can be cut off from inflows.

Fig. 6B shows the Cienega during winter (February 2009). *T. domingensis* was mostly dormant, and fell mainly into the soil/dry

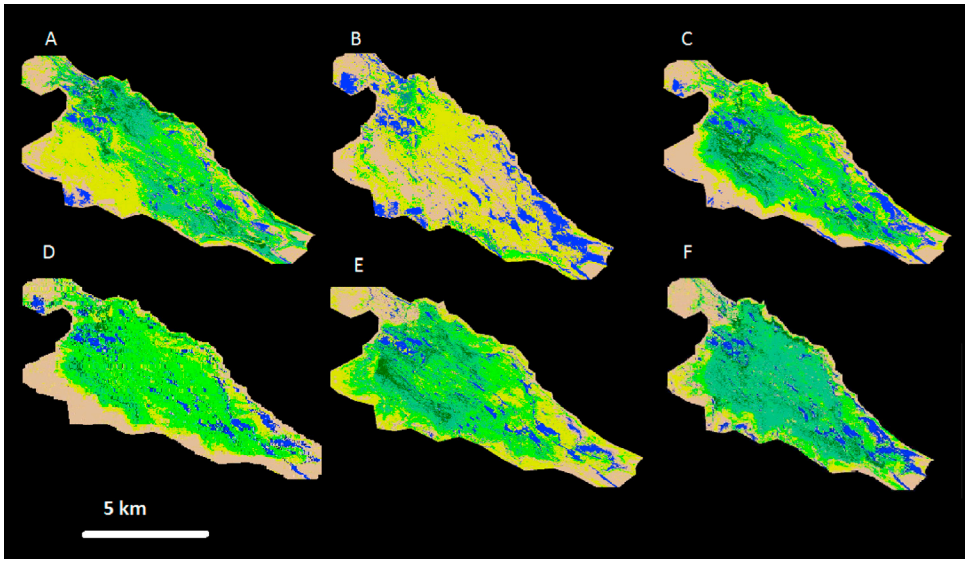

Fig. 6. NDVI-based vegetation density maps of Cienega de Santa Clara on different dates. Images were from September 8, 2008 (A); February 12, 2009 (B); August 19, 2009 (C); July 7, 2010 (D); April 27, 2011 (E); and October 7, 2011 (C).

Table 3
Error matrix and producer's and user's accuracy calculations for Quickbird and WorldView-2 classified images of the Cienega de Santa Clara. Land cover classes are water (W), soil or dry vegetation (S/DT), low-intensity vegetation (LV); medium-intensity vegetation (MV); high-intensity vegetation (HV) and highest-intensity vegetation (HIGHEST). Bolded numbers along the diagonal of the table are the number of reference pixels scored correctly for each; other numbers in rows are pixels that should have been put into a given class but were not, while other numbers in columns are pixels that were erroneously assigned to a given class.

	W	S/DV	LV	MV	HV	HIGHEST	Totals	PROD. %	USER %
W	**57**	0	0	0	0	0	57	100	100
S/DV	0	**111**	4	0	0	0	115	98	97
LV	0	2	**90**	5	0	0	97	92	93
MV	0	0	4	**90**	1	0	95	91	95
HV	0	0	0	4	**27**	3	34	90	79
HIGHEST	0	0	0	0	2	**27**	29	90	93
Totals:	57	113	98	99	30	30	Overall	86	87

vegetation or low vegetation density classes. The green areas denote *P. australis* stands, which are found in shallower areas around the periphery of the marsh and in islands near the entry point of water, where silt accumulates. Note that more open water is visible in winter than summer, as evaporative demand is low in winter. By August 2009 (Fig. 6C), the marsh had re-greened. Dredging had restored part of the western edge of the marsh. Fig. 6D shows the marsh in July 2010, during the test run of the YDP. Although the marsh had greened up normally, most of the vegetation was in the medium-density class, with less high and very-high-density vegetation present compared to September 2008 or August 2009. Fig. 6E shows the Cienega in April 2011, just three weeks after a fire had burned most of the dry vegetation. *T. domingensis* responded by rapidly sending up new green shoots, resulting in early greening compared to previous years. Fig. 6F shows the Cienega in October 2011. Although the image was captured after peak greenness, most of the vegetation fell in the high-density class. Periodic fire burns off thatch in *Typha* marshes, returning nutrients to the water and allowing additional light penetration to support new growth.

Table 4 gives the actual acreage of each cover class for each date. Across images, open water occupied 727 ha of the marsh; from the spring and summer images, bare soil occupied 1235 ha, mainly around the periphery of the vegetated area, as the AOI file encompassing the study are was purposely drawn with a buffer zone to capture areas that were only occasionally vegetated. The area occupied by *P. australis* was roughly inferred from the amount of vegetation in the medium density or higher vegetation classes in winter, and was about 350 ha. Table 1 also gives mean values and coefficients of variation (CV = standard deviation/mean) for each class across images. CVs for water, soil/dry vegetation and total vegetated area were relative low (0.29–0.37) compared to CVs for individual vegetation classes (0.47–0.91). The classification procedure was able to capture the seasonal and inter-annual vegetation dynamics inherent in this type of marsh. Table 1 supports the visual interpretation of the vegetation maps, showing a decrease in the amount of high-density and highest-density vegetation classes during the run of the YDP compared to August 2009, although the differences were not large. Table 1 shows a marked increase in the high-density vegetation classes in 2011 compared to previous years, due to the fire in the spring of that year.

3.3. Flows, salinities and NDVI values from 2000 to 2011

MODIS NDVI values are in Fig. 7A and mean flows and salinities during the May 9 to September 14 period for each year are in Fig. 7B. Salinities were nearly constant from 2000 to 2011 (mean = 2.66 g L^{-1}, CV = 8.7%), but showed a small increase during the YDP test run in 2010. Inflows were more variable (mean = 4.03 m^3 s^{-1}, CV = 16.8%), with distinct interruptions in summer flows noted for 2001 and 2010. In 2001, flows decreased from 4.0 m s^{-1} in May and June, to 1.2 m s^{-1} in July and August, with normal flows restored in September. Flows in 2010 did not decrease to the same low values as in 2010, but the period of flow interruption was longer, with a mean flow of 2.8 m s^{-1} from May 9 to September 14. NDVI values (Fig. 7B) showed the expected annual pattern for vegetation that undergoes winter dormancy, with green-up starting in April, peak greenness occurring in August and September, and senescence of leaves starting in October and November. Peak summer values varied considerably among years. Fires in the spring of 2006 and 2011 burned the dormant *T. domingensis* biomass throughout the marsh, and lead to an early and vigorous green-up in April in both years, with peak NDVI values 30% higher than in non-fire years (Fig. 8). Lowest NDVI values were in the two years of reduced flow (2001 and 2010). The mid-summer interruption in flows in 2001 is clearly evident in the NDVI

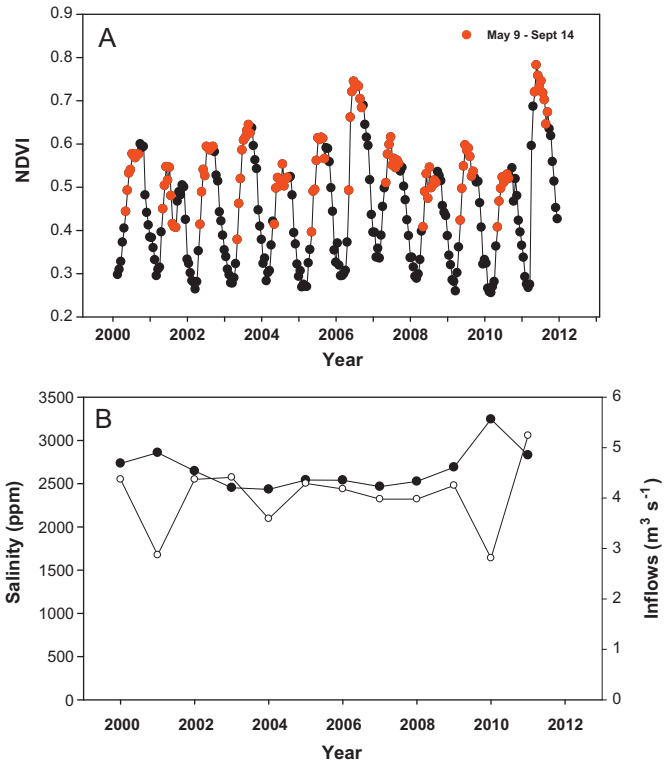

Fig. 7. (A) MODIS NDVI values for vegetation in Cienega de Santa Clara at 16-day intervals, 2000–2011. Red data points show values for the period May 9 to September 14, which corresponds to the period of reduced flows to the Cienega during the 2010 test run of the Yuma Desalting Plant. (B) Salinity (closed circles) and flow volumes (open circles) in the MODE canal during the same period each year. Note that high NDVI values in 2006 and 2011 occurred following spring fires that removed thatch from *T. domingensis* stands.

Table 4
Number of hectares in each cover class in Quickbird or World View 2 images of Ciénega de Santa Clara. "Low", "medium", "high" and "highest" refer to intensity of "greenness" not elevation above the ground. CV, coefficient of variation.

	Month and year									
	Sept. 08	Feb. 09	Apr. 09	Aug. 09	Jan. 10	Apr. 10	July 10	Apr. 11	Oct. 11	Mean (CV)
Water	1007	958	869	543	759	569	465	478	588	723 (29)
Soil/dry veg	1736	2249	1581	1509	1483	474	1682	1087	1228	1448 (34)
Low veg	1886	3027	3786	1335	3991	2569	1442	1952	940	2325 (47)
Medium veg	726	313	257	1311	250	1949	1535	1380	836	951 (65)
High veg	779	92	0	1421	0	820	1261	1296	2535	912 (91)
Highest veg	406	0	45	419	50	154	150	337	407	219 (79)
All veg	3797	3432	4088	4486	4291	5492	4388	4965	4718	4029 (37)

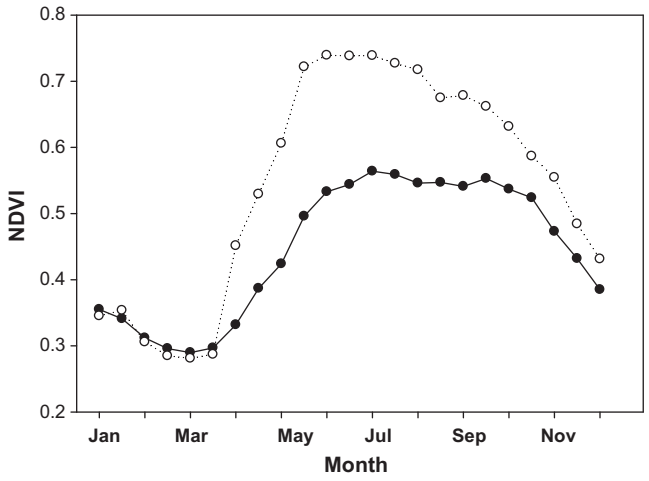

Fig. 8. Phenology of *T. domingensis* growth in Cienega de Santa Clara, showing non-fire years (2000–2005, 2007–2010) (closed circles) and fire years (2006, 2011) (open circles) separately.

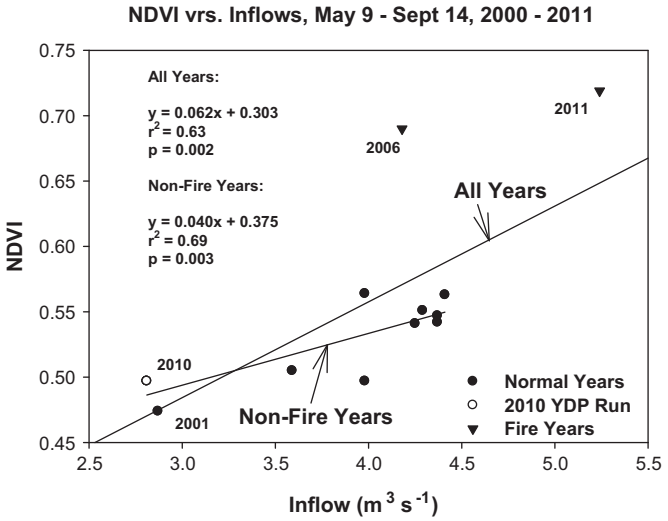

Fig. 9. Linear regression analyses of NDVI values in Cienega de Santa Clara during the period May 9 to September 14, 2000–2011. Fire years are shown separately from non-fire years, and regression equations for all years and for non-fire years only are show separately.

response, which showed a mid-summer dip in NDVI, followed by a recovery in September following restoration of flows (Fig. 7A). The pattern in 2010 was different, with peak NDVI reduced over a longer period but not as deeply as in 2001 (Fig. 7A and Table 5).

A multiple linear regression analysis showed that inflow volumes and presence or absence of fire could explain 95% of the variation in NDVI for the May 9 to September 14 period across years (Table 2) ($P < 0.001$), whereas salinity was not significant ($P = 0.702$). Fig. 9 shows the linear regression of NDVI on flow rates in both fire years and non-fire years. The regression of NDVI on flows was significant ($P < 0.01$) when all years were included in the analysis and when fire years were excluded, but as expected the slope of the response changed. Fig. 9 shows that 2001 and 2010 stand out as years of low flow and low NDVI. Two-way ANOVA of non-fire years shows that 2001 and 2010 differed from other years in both flows ($P < 0.001$) and NDVI ($P = 0.023$).

Table 5
Multiple linear regression of NDVI on inflows in the MODE canal and during the May 9 to September 14 period and presence or absence of fire for years 2000–2011 in Cienega de Santa Clara. The regression equation of best fit was: NDVI = 0.041 Flows ($m\,s^{-1}$) + 0.143 Fire (0 or 1) + 0.369, $F = 85$, $P < 0.001$. The Standard Coefficient expresses the fraction of variability in the dependent variable that is explained by each dependent variable.

Variable	Coefficient	Std. coefficient	*P*
Constant	0.369	0.000	<0.001
Flows	0.041	0.370	0.002
Fire	0.143	0.745	<0.001

4. Discussion

4.1. Advantage of combining high spatial-resolution and high temporal-resolution imagery for change detection

Land cover changes are often assessed on high-resolution image sets (e.g. Landsat) acquired annually, but the efficacy of this approach is limited in complex biological systems (Lunetta et al., 2006). Natural seasonal and inter-annual variations in vegetation density can impede the ability to detect long-term changes when only a few images are compared. As a refinement, Lunetta et al. (2006) combined fine-resolution vegetation maps from the National Land Cover Data set (based on Landsat imagery) with MOSIS 16-day NDVI imagery to detect changes in the Albemarle-Pamlico estuary system on the Atlantic coast of the United States. The combined approach was able to detect land cover changes of under 1% per year, based on phenological differences among years determined by MODIS for specific vegetation units identified on the vegetation maps. The present study also supports the value of the combined approach. While the Quickbird and WorldView-2 images were able to able to accurately classify the Cienega based on land cover types, each image represented only a snapshot of the marsh on a given date, and the marsh vegetation exhibits marked seasonality, complicating efforts to separate seasonal changes from structural changes. On the other hand, MODIS was able to reveal responses to changes in inflows and effects of

fire based on time-series imagery, with 23 scenes per year available using the MODQ13Q1 NDVI product.

4.2. Land cover classes in Cienega de Santa Clara

It needs to be noted that the high Producer's and User's Accuracy achieved in this study was partly due to lack of independence of reference and validation data (Congalton, 1991). Reference sites for water and soil were selected independently of NDVI, but the different green vegetation classes were determined by their NDVI values, hence good agreement between reference and validation data is expected. Nevertheless, NDVI was an appropriate method for classifying vegetation in this study because it is related to such factors as leaf area index and photosynthesis, which could be impacted by operation of the YDP or other environmental factors. Vegetation maps from 2009 to 2011 show that the overall size of the Cienega is stable at about 5600 ha. Open water accounts for about 15% of the surface area, mainly in the form of lagoons within the *T. domigensis* and *P. australis* stands, but also as transient drainage channels from the periphery onto the mudflats to the west and south of the Cienega. The open water lagoons are stable features and appear to be areas of deeper water where *T. domingensis* has not established. These lagoons are colonized by dense growth of the submerged aquatic species, *Najas marina*, which might prevent the establishment of emergent plants, explaining the stability of the lagoons over time. The islands of *P. australis* within the *T. domingensis* stands also appear to be stable features. *P. australis* preferentially grows in shallow water areas, and is most abundant along the margins of the Cienega and near the entry point for water at the north end of the Cienega on silt bars that have built up over time. Silt entering the Cienega is accumulating near the entry point for water and, although most of the vegetation units are stable over time, the western edge is prone to periodic dry-downs due to silt build up in the distribution canal, and must be restored through periodic dredging, as captured in the Quickbird series of images in this study.

4.3. Main anthropogenic factors controlling the extent and density of vegetation in the Cienega

Presence or absence of fire and water inflow rates were both significant factors controlling the density of green vegetation in spring and summer, as estimated by NDVI values on MODIS images. Fires in spring of 2006 and 2011 removed accumulated thatch and returned nutrients to the water (see Liu et al., 2010), resulting in a marked increase in NDVI values the following summer. Fires markedly improve the habitat value of *Typha* marshes for nesting birds, as noted in other studies (Conway et al., 2010). Yuma clapper rail densities were significantly correlated with NDVI values during the nesting period in Cienega de Santa Clara. Fire timing and frequency appears to be self-limiting in *Typha* marshes. Fires require high thatch levels as fuel, hence newly greened marshes or marshes in summer might not be prone to burning. Fires occur mainly in winter and early spring and are most intense when thatch levels are high. *Typha* grows by initiating new shoots from rhizomes in spring, but the previous year's senescent leaves are retained on the plant, leading to the accumulation of thatch over multiple years that is periodically removed by fire. In the Cienega, fires are sometimes deliberately set by local residents to allow fishermen and hunters easier access to areas within the marsh, and can also be started by lightning strikes.

Flows control vegetation density by determining the flooded area available for the growth of emergent vegetation, and the amount of water available for evapotranspiration and growth. Flows in the MODE tended to be fairly constant during most years from 2000 to 2011, but reduced summer flows in 2001 and 2010 led to reductions in marsh NDVI, and the regression of NDVI on flows was significant ($P < 0.01$) across all years.

Although not a significant factor in the multiple regression analysis, salinity is also a determinant of vegetation density in the Cienega (Huckelbridge et al., 2010). Both greenhouse studies (Glenn et al., 1995) and field observations (Glenn et al., 1995) show that *T. domingensis* exhibits a linear decrease in growth with salinity over the range of $0\,g\,L^{-1}$ total dissolved salts (TDS) (i.e., fresh water), and $6\,g\,L^{-1}$ TDS, the apparent upper limit for growth. *T. domingensis* survives at salinities up to $8\,g\,L^{-1}$, but growth rates approach zero at $6\,g\,L^{-1}$ in greenhouse experiments, which is also the apparent salinity limit for the distribution of *T. domingensis* in the Cienega de Santa Clara (Glenn et al., 1995).

4.4. Other factors impacting the Cienega vegetation

The Ciénega is located in a dynamic environment subject to complex interactions of tectonic, fluvial, and tidal forces at the head of the Gulf of California (Thompson, 1986; Nelson et al., submitted for publication). Several high tides per year reach the southern and western periphery of the Cienega, although they do not seem to affect the vegetation in the Cienega. Although the Cienega is normally separated from the fresh water wetlands bordering the Hardy and Colorado rivers to the west, the Ciénega was briefly connected to these wetlands in the early 1980s when river flood waters were temporarily impounded behind a tidal sand bar obstructing the estuary channel. The Ciénega is also bisected by the Cerro Prieto transform fault, which was the site of a 7.2 earthquake in 2010. Although this earthquake did not appreciably affect the Cienega, it caused changes in the drainage patterns in the intertidal zone adjacent to the Cienega (Nelson et al., submitted for publication). The Cienega could also be impacted by sea level rise, which could increase the tidal exchange and therefore the salinity of the wetland, perhaps leading to a decrease in *T. domingensis* and an increase in more salt-tolerant emergent plants. Hence, as with other coastal wetland systems (Kearney and Riter, 2011; Penland and Ramsey, 1990), the Cienega is part of a dynamic estuary and is subject to change from a number of forces over time. Given its importance in supporting wildlife and its status as a protected wetland in a Biosphere Reserve, continued monitoring via satellite imagery and ground surveys will be needed to assess the status of the Cienega in the years to come.

4.5. Comparison to other studies

There is continuing debate about the controls on wetland productivity and whether marshes are profligate water users (Goulden et al., 2007). In some studies productivity of *Typha* spp. is high and evapotranspiration (ET) rates equal or exceed open water evaporation rates (Farnsworth and Meyerson, 2003; Towler et al., 2004; Drexler et al., 2008). However, other studies report more modest rates of ET and net primary production for *Typha* marshes (Goulden et al., 2007). The present study shows that the amount of thatch largely controls the NDVI and ET in Cienega de Santa Clara. In restored marshes (Drexler et al., 2008) or lysimeter studies (Towler et al., 2004) ET rates tend to be high, because plants are maintained for maximum productivity. On the other hand, in natural marsh, thatch will unavoidably build up over time, reducing light levels inside the canopy and sequestering nutrients in senescent biomass (Goulden et al., 2007). Fig. 8 shows that total seasonal NDVI (areas under curves) was nearly twice as great after fires compared to non-fire years in the Cienega. We postulate that much of the variation in ET and NPP rates noted in the literature for *Typha* wetlands could

be due to differences in experimental conditions, in particular to how much thatch is present during measurement periods.

4.6. Need for a mechanistic model of vegetation versus flows, fire and salinity levels in the Cienega

The multiple linear regression equation in Table 2 identifies the roles of fire and flow rates in controlling vegetation density, but does not constitute a model of vegetation dynamics in the Cienega. The equation is only predictive over the range of conditions occurring from 2000 to 2011. Thus, salinity does not appear as a significant factor in the equation because it did not vary greatly, but proposed operating scenarios for the YDP do include significant increases in inflow salinities. Furthermore, the dips in NDVI in response to flow reductions in 2001 and 2011 are rather small, due to the transient nature of the flow reductions. More prolonged reductions in flow would be expected to reduce NDVI or marsh area more substantially than noted in this study. The multiple linear regression equation treats fire and flows as separate variables, but in reality an interaction between flows, salinities and presence or absence of fire is expected. Although not done in this study, it should be possible to correlate NDVI values with the percentage of dry thatch present in the *T. domingensis* stands by combining ground harvests of thatch and green shoots with Quickbird and MODIS NDVI imagery; this would produce a more quantitative measurement of thatch accumulation than NDVI alone can provide.

The preliminary model formulated by Huckelbridge et al. (2010) can now be refined using data gathered during the 2008–2011 monitoring program (Greenberg and Schlatter, 2012), to provide a validated tool for predicting the vegetation and hydrological response of the Cienega to alterations in inflows and salinities.

References

Baldi, G., Nosetto, M.D., Aragon, R., Aversa, F., Paruelo, J.M., Jobbagy, E.T., 2008. Long-term satellite NDVI data sets: evaluating their ability to detect ecosystem functional changes in South America. Sensors 8, 5397–5425.

Cohen, J., 1960. A coefficient of agreement for nominal scales. Educ. Phychol. Meas. 20, 37–46.

Congalton, R.G., 1991. A review of assessing the accuracy of classifications of remotely sensed data. Remote Sens. Environ 37, 35–46.

Conway, C.J., Nadeau, C.P., Priest, L., 2010. Fire helps restore natural disturbance regime to benefit rate and endangered marsh birds endemic to the Colorado River. Ecol. Appl. 20, 2024–2035.

Digital Globe, Inc., 2006. Quickbird Imagery Products. Digital Globe, Inc., Longmont, CO. Available on-line at: http://glcf.umiacs.umd.edu/library/guide/QuickBird_Product_Guide.pdf.

Drexler, J.Z., Anderson, F.E., Snyder, R.L., 2008. Evapotranspiration rates and crop coefficients for a restored marsh in the Sacramento-San Joaquin Delta, California, USA. Hydrol. Process. 22, 725–735.

Farnsworth, E.J., Meyerson, L.A., 2003. Comparative ecophysiology of four wetland plant species along a continuum of invasiveness. Wetlands 23, 750–762.

Gabriel, J., Kelli, L., 2010. The Yuma desalting plant and Cienega de Santa Clara dispute: a case study review of a workgroup process. Water Policy 12, 401–415.

Garcia-Hernandez, J., Glenn, E.P., Artiola, J., 2000. Bioaccumulation of selenium (Se) in the Cienega de Santa Clara wetland, Sonora, Mexico. Ecotoxol. Environ. Saf. 46, 298–304.

Glenn, E.P., Felger, R.S., Burquez, A., Turner, D.S., 1992. Cienega de Santa Clara—endangered wetland in the Colorado River Delta, Sonora, Mexico. Nat. Res. J. 32, 817–824.

Glenn, E.P., Huete, A.R., Nagler, P.L., Nelson, S.G., 2008. Relationship between remotely-sensed vegetation indices, canopy attributes and plant physiological processes: what vegetation indices can and cannot tell us about the landscape. Sensors 8, 2136–2160.

Glenn, E., Thompson, T.L., Frye, R., Riley, J., Baumgartner, D., 1995. Effects of salinity on growth and evapotranspiration of *Typha domingensis* Pers. Aquat. Bot. 52, 75–91.

Glenn, E.P., Zamora-Arroyo, F., Nagler, P.L., 2001. Ecology and conservation biology of the Colorado River delta, Mexico. J. Arid Environ. 49, 5–15.

Goulden, M.L., Livak, M., Miller, S.D., 2007. Factors that control *Typha* marsh evapotranspiration. Aquat. Bot. 86, 97–106.

Greenberg, K., Schlatter, K. (Eds.), 2012. Monitoring Program for the Cienega de Santa Clara. International Boundary and Water Commission. El Paso, Texas.

Hinojosa-Huerta, O., DeStefano, S., Shaw, W.W., 2002. Evaluation of call-response surveys for monitoring breeding Yuma Clapper Rails (*Rallus longirostris yumanensis*). J. Field Ornith. 73, 151–155.

Hinojosa-Huerta, O., DeStefano, S., Shaw, W.W., 2001. Distribution and abundance of the Yuma clapper rail (*Rallus longirostris yumanensis*) in the Colorado River delta, Mexico. J. Arid Environ. 49, 171–182.

Huckelbridge, K.H., Stacey, M.T., Glenn, E.P., Dracup, J.A., 2010. An integrated model for evaluation hydrology, hydrodynamics, salinity and vegetation cover in a coastal desert wetland. Ecol. Eng. 36, 850–861.

Huete, A., Didan, K., van Leeuwen, W., Miura, T., Glenn, E., 2011. MODIS vegetation indices. Land Rem. Sens. Environ. Change 11, 579–602.

Jensen, J.R., 2000. Remote Sensing of the Environment: An Earth Resource Perspective. Prentice Hall Upper Saddle River, New Jersey, 544pp.

Kearney, M.S., Riter, J.C.A., 2011. Inter-annual variability in Delaware Bay brackish marsh vegetation, USA. Wetlands Ecol. Manage. 19, 373–388.

Kerr, J., Ostrovsky, M., 2003. From space to species: ecological applications for remote sensing. Trends Ecol. Evol. 18, 299–305.

Krause, K., 2005. Radiometric use of Quickbird Imagery. Digital Globe, Longmont, CO, USA, http://www.digitalglobe.com/downloads/QuickBird_technote_raduse_v1.pdf.

Liu, G.D., Ga, B., Miao, S.L., Li, Y.C., Migliaccio, K.W., Qian, Y., 2010. Phosphorous release from ash and remaining tissues of two wetland species after a prescribed fire. J. Environ. Qual. 39, 1585–1593.

Lunetta, R.S., Knight, J.F., Ediriwickrema, J., Lyon, J.G., Worthy, L.D., 2006. Land cover change using multi-temporal <ODIS NDVI data. Remote Sens. Environ. 105, 142–154.

Muller, E., 1997. Mapping riparian vegetation along rivers: old concepts and new methods. Aquat. Bot. 58, 411–437.

Nagler, P.L., Glenn, E.P., Hursh, K., Curtis, C., Huete, A., 2009a. Vegetation mapping for change detection on an arid-zone river. Environ. Monitor. Assess. 109, 255–274.

Nagler, P.L., Glenn, E.P., Hinojosa-Huerta, O., 2009b. Synthesis of ground and remote sensing data for monitoring ecosystem functions in the Colorado River Delta, Mexico. Rem. Sens. Environ. 113, 1473–1485.

Nelson, S., Fielding, E., Zamora-Arroyo, F., Flessa, K. Delta dynamics: effects of tides, river flows and a major earthquake on Ciénega de Santa Clara and the Colorado River delta, Mexico. Ecol. Eng., submitted for publication.

Penland, S., Ramsey, K.E., 1990. Relative sea-level rise in Louisiana and the Gulf of Mexico: 1908–1988. J. Coast. Res. 6, 323–342.

Pettorelli, N., Vik, J., Mysterud, A., Caillard, J., Tucker, C., Stenseth, N., 2005. Using the satellite-derived NDVI to assess ecological responses to environmental change. Trends Ecol. Evol. 20, 503–510.

Thompson, R.W., 1986. Tidal Flat Sedimentation on the Colorado River Delta, Northwestern Gulf of California. Geolog. Soc. Am. Memoir, p. 107.

Towler, B.W., Cahoon, J.E., Stein, O.R., 2004. Evapotranspiration crop coefficients for cattail and bulrush. J. Hyrdol. Eng. 9, 235–239.

Updike, T., Comp, C., 2010. Radiometric Use of WorldView-2 Imagery. Digital Globe, Inc., Longmont, CO, Available on-line at: http://www.digitalglobe.com/downloads/Radiometric_Use_of_WorldView-2_Imagery.pdf.

Verbesselt, J., Hyndman, R., Newnham, G., Culvenor, D., 2010. Detecting trend and seasonal change in satellite time series. Rem. Sens. Environ. 114, 106–115.

Xie, Y., Sha, Z.G., Yu, M., 2008. Remote sensing imagery in vegetation mapping: a review. J. Plant Ecol. 1, 9–23.

Zengel, S.A., Glenn, E.P., 1996. Presence oft he endangered desert pupfish (*Cyprinodon macularius*, Cyprinidontidae) in Cienega de Santa Clara, Mexico, following an extensive marsh dry-down. Southwest Nat. 41, 73–78.

Zengel, S.A., Meretsky, V.J., Glenn, E.P., Felger, R.S., Ortiz, D., 1995. Cienega de Santa Clara, a remnant wetland in the Rio Colorado delta (Mexico)—vegetation distribution and the effects of water flow reduction. Ecol. Eng. 4, 19–36.